Parametric Doppler Spread Estimation in Mobile Fading Channels

Mingzheng Cao, Hongya Ge, Hong Zhang† and Ali Abdi
Department of Electrical and Computer Engineering
New Jersey Institute of Technology
Newark, New Jersey 07102, USA
†InterDigital Communications Corporation
781 Third Avenue, King of Prussia, Pennsylvania 19406, USA
Email: {mc229, ge, ali.abdi}@njit.edu, †hong.zhang@ieee.org

***Abstract*— In this work, a parametric method is proposed to estimate the Doppler spread, or the mobile speed by modeling the received data at the base station as an autoregressive process. The method can be extended to a spatial-temporal parametric Doppler spread estimator when multiple antennas are available at the base station. Compared to the nonparametric estimator based on periodogram method, the parametric estimator can achieve a higher resolution, providing more accurate mobile speed information without increasing the computation complexity.**

I. Introduction

The Doppler spread, or equivalently, the mobile speed, is a measure of the spectral dispersion of a mobile fading channel. Accurate estimation of the mobile speed, or the maximum Doppler frequency, which indicates the rate of wireless mobile channel variations, is important for many applications such as handoff, adaptive modulation and equalization, power control [1] [2], etc. In [1], a nonparametric mobile speed estimator based on the periodogram method is proposed by exploiting the unique feature of the Doppler spectrum of mobile fading channels. Compared with conventional crossing-based and covariance-based speed estimator, this technique is not only robust against the noise, but also insensitive to nonisotropic scattering observed at the mobile station (MS), providing significant performance improvement. In [2] the estimator based on periodogram method is extended from temporal-only speed estimator of [1] to a spatio-temporal estimator, using multiple antennas at the base station (BS) of macrocell-type environments. From a signal precessing aspect, the proposed speed estimators in [1] [2] are related to the spectral analysis problem. Compared to the nonparametric spectral analysis methods, parametric methods have advantages in providing better resolution of multiple spectral lines or other narrow features when the amount of data is severely limited, and providing repeatable experiment so that an ensemble of data segments is available [3]. In this work, a parametric doppler spread estimator is proposed by modeling the received data at the base station as an autoregressive (AR) process. By implementing Levinson-Durbin algorithm, the parametric doppler spread estimator is computationally competitive with periodogram method based on Fast Fourier Transform (FFT) [3]. The proposed estimator can be extended to a spatial-temporal parametric Doppler spread estimator when multiple antennas are available at the base station. Simulation results show that compared to the periodogram method, the parametric estimator can achieve a higher resolution, providing more accurate mobile speed information.

II. The Channel Model

The received lowpass complex envelope at the base station (BS) with a single antenna in a noisy Ricean frequency-flat fading channel, in response to an unmodulated carrier transmitted from the mobile station (MS), is given as

$$y(t) = s(t) + n(t), \tag{1}$$

where $n(t)$ represents the additive noise and the complex process $s(t)$ includes the random diffuse component $h(t)$ and the deterministic line-of-sight (LOS) component. In a two dimensional (2D) propagation environment, where the probability density function (PDF) of the angle-of-arrival (AOA) in the elevation plane is chosen as $p(\zeta) = \delta(\zeta - \frac{\pi}{2})$ (In this paper $\delta(\cdot)$ denotes the Dirac delta function), $s(t)$ can be given as

$$s(t) = \sqrt{\frac{P_s}{K+1}}h(t) + \sqrt{\frac{KP_s}{K+1}}\exp\{-j(2\pi f_d t\cos\alpha_0 + \varphi_0)\}, \tag{2}$$

where $P_s = E[|s(t)|^2]$ is the average signal power, and the Ricean factor K is the ratio of the LOS power to the diffuse power. $f_d = \frac{\nu}{\lambda} = \frac{\nu f_c}{c}$ is the maximum Doppler frequency in Hz, ν is the MS speed, λ is the wavelength, f_c is the carrier frequency, and c is the speed of light. Furthermore, $j = \sqrt{-1}$, α_0 and φ_0 stand for AOA in the azimuth plane and the phase of the LOS component at BS, respectively.

The random diffuse component $h(t)$ can be represented as

$$h(t) = \lim_{M\to\infty}\frac{1}{\sqrt{M}}\sum_{m=1}^{M} a_m \exp\{-j(2\pi f_d t\cos\theta_m + \varphi_m)\}, \tag{3}$$

where $\{a_m\}_{m=1}^M$ are normalized complex constants satisfying $\lim_{M\to\infty}\frac{1}{\sqrt{M}}\sum_{m=1}^M |a_m|^2 = 1$, $\{\theta_m\}_{m=1}^M$ are independent and identically distributed (i.i.d.) angles that the incoming waves make with the mobile direction, with PDF $p(\theta)$ in the azimuth plane, and $\{\varphi_m\}_{m=1}^M$ are i.i.d. phase uniformly distributed on $[0, 2\pi)$, respectively. Assuming when M is large, $h(t) \sim \mathcal{CN}(0,1)$.

The autocorrelation function of $s(t)$ is defined as $r_s(\tau) = E[s(t)s^*(t+\tau)]$ with $*$ denoting complex conjugate. With unit-gain isotropic receive antenna and incorporating the effect of θ, using von Mises PDF $p(\theta) = \exp\{\kappa\cos(\theta-\alpha)\}/(2\pi I_0(\kappa))$, $r_s(\tau)$ can be written as [5]

$$r_s(\tau) = \frac{P_s}{K+1}\frac{I_0\Big(\sqrt{\kappa^2 - 4\pi f_d^2\tau^2 + j4\pi\kappa f_d\tau\cos\alpha}\Big)}{I_0(\kappa)} + \frac{KP_s}{K+1}\exp\{j2\pi f_d\tau\cos\alpha_0\}, \quad (4)$$

where $\alpha \in [0, 2\pi)$ is the mean direction of the azimuth AOA, $\kappa \geq 0$ determines the width of the azimuth AOA, and $I_0(\cdot)$ is the zero-order modified Bessel function of the first kind. Consequently, the power spectral density (PSD) of $s(t)$ can be given by [5]

$$\Omega_s(f) = \frac{P_s}{K+1}\frac{\exp\{\frac{\kappa f\cos\alpha}{f_d}\}\cosh\Big(\kappa\sin\alpha\sqrt{1-(\frac{f}{f_d})^2}\Big)}{I_0(\kappa)\pi\sqrt{f_d^2 - f^2}} + \frac{KP_s}{K+1}\delta(f + f_d\cos\alpha_0), \qquad |f| \leq f_d \quad (5)$$

where $\cosh(\cdot)$ is the hyperbolic cosine function. When $K = 0$, $\kappa = 0$, $r_s(\tau) = P_s J_0(2\pi f_d\tau)$, where $J_0(\cdot)$ is the zero-order Bessel function of the first kind, (4) reduces to the classic Clarke's model. For Clarke's model, (5) reduces to the well-known U-shape Doppler spectrum given as [6]

$$\Omega_s(f) = P_s\pi^{-1}(f_d^2 - f^2)^{-\frac{1}{2}}. \qquad |f| \leq f_d \quad (6)$$

By including the incoming waveforms from the elevation plane, the three dimensional (3D) AOA model can be established. Assuming the azimuth and elevation AOA's are uniformly distributed over $[-\pi, \pi)$ and $[\frac{\pi}{2} - \beta, \frac{\pi}{2} + \beta]$ with $\beta \in [0, \frac{\pi}{2})$, respectively, then $r_s(\tau)$ becomes [1]

$$r_s(\tau) = \frac{P_s}{K+1}\frac{1}{2\sin\beta}\int_{\frac{\pi}{2}-\beta}^{\frac{\pi}{2}+\beta} J_0(2\pi f_d\tau\sin\zeta)\sin\zeta\,\mathrm{d}\zeta + \frac{KP_s}{K+1}\exp\{j2\pi f_d\tau\cos\alpha_0\sin\beta_0\}. \quad (7)$$

The corresponding PSD of $s(t)$ for 3D AOA model is [1]

$$\Omega_s(f) = \frac{P_s}{K+1}\Omega_h(f) + \frac{KP_s}{K+1}\delta(f + f_d\cos\alpha_0\sin\beta_0), \quad (8)$$

where

$$\Omega_h(f) = \begin{cases} \dfrac{\sin^{-1}\left(\frac{\sin\beta}{\cos[\sin^{-1}(f/f_d)]}\right)}{\pi f_d\sin\beta}, & 0 \leq |f| < f_d\cos\beta \\ \dfrac{1}{2f_d\sin\beta}, & f_d\cos\beta \leq |f| \leq f_d \end{cases}.$$

III. The Parametric Speed Estimation

Since there are two singularities at $f = \pm f_d$ of the basic fading spectrum with the 2D isotropic scattering in (6), and the peak of $\Omega_s(f)$ at the maximum Doppler frequency exists, irrespective of the nonisotropic scattering, 3D propagation model and PDF of the noise. Consequently, the estimated Doppler spread $\hat{f}_d$ is the frequency at which the estimated spectrum of the sampled data $y[n]$ of (1) achieves its maximum [1]. In [1] [2], the periodogram based nonparametric spectrum estimation technique is chosen due to its simplicity. In this paper, we model the sampled data $y[n]$ as a discrete AR process. By implementing the Levinson-Durbin algorithm [3] [4], the parametric Doppler spread estimator is computationally competitive with periodogram method, but provides more accurate mobile speed information with limited amount of data.

Denote $\{y[n]\}_{n=0}^{N-1}$ as the N samples of $y(t)$ within duration T. The Pth order AR model of the time-series $y[n]$ is the difference equation

$$y[n] + a_1 y[n-1] + \cdots + a_P y[n-P] = bv[n], \quad (9)$$

where $v[n] \sim \mathcal{CN}(0,1)$. Following the same autocorrelation definition as $r_s(\tau) = E[s(t)s^*(t+\tau)]$ for consistence, the autocorrelation function $r_y(k) = E\{y[n]y^*[n+k]\}$ can be estimated by means of the time-average formula

$$\hat{r}_y(k) = \frac{1}{N}\sum_{n=0}^{N-k-1} y[n]y^*[n+k]. \qquad k = 0, 1, \ldots, P \quad (10)$$

The AR parameters $\{a_p\}_{p=1}^P$ can be obtained by solving the Yule-Walker equations given by [4]

$$\begin{bmatrix} \hat{r}_y(0) & \hat{r}_y(1) & \cdots & \hat{r}_y(P-1) \\ \hat{r}_y^*(1) & \hat{r}_y(0) & \cdots & \hat{r}_y(P-2) \\ \vdots & \vdots & \ddots & \vdots \\ \hat{r}_y^*(P-1) & \hat{r}_y^*(P-2) & \cdots & \hat{r}_y(0) \end{bmatrix}\begin{bmatrix} -a_1 \\ -a_2 \\ \vdots \\ -a_P \end{bmatrix} = \begin{bmatrix} \hat{r}_y^*(1) \\ \hat{r}_y^*(2) \\ \vdots \\ \hat{r}_y^*(P) \end{bmatrix}.$$

The Yule-Walker equations can be efficiently solved by implementing Levinson-Durbin algorithm. The details of the algorithm can be found in [3] [7]. Once the AR parameters $\{a_p\}_{p=1}^P$ are available, the PSD for $y[n]$ can be obtained as

$$S_y(f') = \frac{b^2}{\left|1 + \sum_{p=1}^P a_p(e^{-j2\pi f'})^p\right|^2}. \qquad |f'| \leq \frac{1}{2} \quad (11)$$

In the absence of aliasing, $S_y(f')$ is the scaled version of the PSD of the continuous $y(t)$, $\Omega_y(f)$, given by [8]

$$S_y(f') = f_s \Omega_y(f' f_s), \qquad |f'| \le \frac{1}{2} \tag{12}$$

where $f_s = \frac{N}{T}$ is the sampling frequency. The parametric Doppler spread estimator is given as

$$\hat{f}_d = f_s |\arg\max_{f'} S_y(f')|. \tag{13}$$

Although parametric method based on AR model can provide superior spectral resolution performance compared to periodogram method, there is a fundamental trade-off between resolution and reliability. In practice some order-determining criteria by employing the sum of squared prediction errors, such as final prediction error criterion (FPE), type A information criterion (AIC), and autoregressive transfer function criterion (CAT) can be used [3].

IV. The Space-Time Parametric Speed Estimation

The proposed estimator can be extended to a spatial-temporal parametric Doppler spread estimator. Considering there is a uniform linear array (ULA) with L omnidirectional unit-gain antennas at BS, the received lowpass complex envelop at the l-th antenna of BS in a noisy Ricean frequency-flat fading channel, in response to an unmodulated carrier transmitted from MS, is

$$y_l(t) = s_l(t) + n_l(t). \qquad l = 1, 2, \ldots, L \tag{14}$$

In a 2D propagation environment, $s_l(t)$ can be represented as [2]

$$\begin{aligned} s_l(t) = & \sqrt{\frac{P_s}{K+1}} h_l(t) + \sqrt{\frac{KP_s}{K+1}} \exp\{-j2\pi f_d t \cos\alpha_0\} \\ & \times \exp\{j2\pi(l-1)(d/\lambda)\cos\alpha_0 + j\varphi_0\}, \end{aligned} \tag{15}$$

where d is the spacing between adjacent antennas. Assuming the azimuth AOA θ has von Mises distribution, the space-time crosscorrelation function between the received signals at the a-th and b-th elements, defined by $r_s((b-a)\Delta, \tau) = E[s_a(t) s_b^*(t+\tau)]$ with $\Delta = d/\lambda$, is derived as [9]

$$\begin{aligned} r_s((b-a)\Delta, \tau) = & \frac{KP_s}{K+1} \exp\{j(u+v)\cos\alpha_0\} + \frac{P_s}{K+1} \\ & \times \frac{I_0\left(\sqrt{\kappa^2 - u^2 - v^2 - 2uv + j2\kappa(u+v)\cos\alpha}\right)}{I_0(\kappa)}, \end{aligned} \tag{16}$$

where $u = 2\pi f_d \tau$, $v = 2\pi(a-b)\Delta$ with $1 \le a \le b \le L$. In a heavily nonisotropic scattering environments where the angle spread at BS is generally small and κ takes large value, the PDF of the diffuse AOA at BS, $p(\theta)$, can be approximated by a Gaussian distribution with mean α and variance $\frac{1}{\kappa}$ [9]. In this case, it is reasonable to assume $\alpha_0 = \alpha$. By setting $\tau = 0$ in (16) and assuming $\{n_l(t)\}_{l=1}^L$ are independent, the spatial cross-correlation function $r_y((b-a)\Delta, 0) = E[y_a(t) y_b^*(t)]$ can be approximated by [9]

$$r_y((b-a)\Delta, 0) \approx \frac{P_s \exp(-\frac{v^2 \sin^2\alpha}{2\kappa}) + KP_s}{K+1} \exp\{jv\cos\alpha\}, \tag{17}$$

For large κ, PSD of $h_l(t)$, $\Omega_{h_l}(f)$ can be written as [2]

$$\Omega_{h_l}(f) \approx P_s \sqrt{\frac{\kappa}{2\pi(f_d^2 - f^2)}} \exp\Big\{ -\frac{\kappa(\cos^{-1}(\frac{f}{f_d}) - \alpha)^2}{2} \Big\}, \tag{18}$$

where positive α and θ are chosen. It achieves its maximum around $f_{l,\alpha} = f_d \cos\alpha$ [2]. Similarly, we model the received signal $y_l(t)$ in (14) as an AR process, and the AR parameters $\{a_{l,p}\}_{p=1}^P$ can be obtained by the N samples of $y_l(t)$, $\{y_l[n]\}_{n=0}^{N-1}$ within duration T. Once the AR parameters $\{a_{l,p}\}_{p=1}^P$ are available, the PSD of $y_l[n]$, $S_{y_l}(f')$ can be obtained. Consequently, the $\hat{f}_{l,\alpha}$ can be obtained by using the proposed method in the previous section as

$$\hat{f}_{l,\alpha} = f_s |\arg\max_{f'} S_{y_l}(f')|. \qquad l = 1, 2, \ldots, L \tag{19}$$

From (17) $\cos\alpha$ can be estimated via

$$\widehat{\cos\alpha} = \frac{\measuredangle \hat{r}_y(\Delta, 0)}{-2\pi\Delta}, \tag{20}$$

where $\measuredangle$ denotes the phase of a complex value and $\hat{r}_y(\Delta, 0)$ is the estimate of $r_y(\Delta, 0) = E[y_a(t) y_{a+1}^*(t)]$, $\forall a \in [1, L-1]$, given by

$$\hat{r}_y(\Delta, 0) = \frac{1}{L-1} \sum_{l=1}^{L-1} \hat{r}_{y_l}(\Delta, 0), \tag{21}$$

where $\hat{r}_{y_l}(\Delta, 0) = \frac{1}{N} \sum_{n=0}^{N-1} y_l[n] y_{l+1}^*[n]$, $l \in [1, L-1]$, is the l-th adjacent antenna pair estimate of $r_y(\Delta, 0)$.

Consequently, f_d can be estimated by

$$\hat{f}_d = \frac{\hat{f}_\alpha}{\widehat{\cos\alpha}}, \tag{22}$$

where $\hat{f}_\alpha = \frac{1}{L} \sum_{l=1}^L \hat{f}_{l,\alpha}$. $\hat{f}_{l,\alpha}$ and $\widehat{\cos\alpha}$ are given in (19) and (20), respectively.

V. Simulation Results

In the simulations, 500 independent realizations of a zero-mean complex Gaussian process are generated using the spectral method [10], with $N = 256$ samples per realization, over $T = 1$ second. The noise is bandlimited Gaussian with a flat spectrum. The average noise power is P_n, and SNR $= \frac{P_s}{P_n}$. Assuming the largest possible Doppler spread f_d is 125 Hz, and the receiver bandwidth is fixed at 125 Hz.

Fig.1 demonstrates that the estimated PSD of the received data at BS based on the AR model matches the theoretic U-shape doppler spectrum of Clark's model very well when $K = 0$, $\kappa = 0$, $\alpha = 0°$ and doppler spread $f_d = 65$ Hz. Here only the positive frequency part is given due to symmetry of the

spectrum, and theoretic PSD is obtained based on (6) without noise while the PSD estimates are obtained when SNR $=$ 10 dB. It can be observed that the frequency to achieve the maximum of PSD moves from 61 Hz to 65 Hz when order P increases from 5 to 35. Consequently, $P = 35$ is chosen to obtain Fig.3 $\sim$ Fig.5. Fig.2 shows that the prediction error decreases monotonically when order P increases.

Fig.3 (a) and Fig.4 (a) are obtained in a 2D isotropic scattering propagation environment and Fig.5 is obtained in a 3D propagation environment. It should be noted that the information of both positive and negative frequency is used due to the symmetry of the spectrum to improve the performance when $K = 0$ and $\kappa = 0$, as seen in (6) and (8), respectively. It can be seen that the parametric estimator based on the AR model has lower root mean squared error (RMSE), providing more reliable Doppler spread estimate than periodogram method. In addition, the parametric estimator also provides more reliable estimate in nonisotropic scattering environment, as shown in Fig.3 (b) and Fig.4 (b) when $K = 0$, $\kappa = 5$ and $\alpha = 36°$.

Fig.6 demonstrates the PSD estimates of the received data at BS based on the AR model and the periodogram method, matching the theoretic spectrum when $K = 0$, $\kappa = 100$, $\alpha = 60°$ and Doppler spread $f_d = 80$ Hz. Here only the positive frequency part is given for simplicity, and theoretic PSD is obtained based on (18) without noise while the PSD estimates are obtained when SNR $= 10$ dB. It should be noted that the frequency to achieve the maximum PSD is around $f_d \cos\alpha = 40$ Hz. It can be observed that the frequency to achieve the maximum of the PSD based on AR model moves to 40 Hz when order $P = 2$, which is chosen to obtain Fig.7 and Fig.8.

When multiple antennas at BS are available, significant performance improvement can be obtained by using spatial information to estimate $\cos\alpha$ as L changes from 1 to 2, but further increase of L does not result in much performance gain [2]. Consequently, only $L = 2$ is considered in the simulations. The space-time parametric method provides superior performance compared to the space-time estimator based on periodogram method in large Doppler spread scenario, as shown in Fig.7. Fig.8 shows RMSE of proposed method is 3 Hz lower than that of the periodogram method when SNR is larger than 5 dB.

VI. Conclusion

This paper investigates the feasibility of a parametric Doppler spread estimator by modeling the received data at BS as an AR process. The proposed parametric estimator can be extended to a space-time parametric Doppler spread estimator by taking advantage of the spatial information when multiple antennas at BS are available. Simulation results show that the parametric estimator can provide more reliable speed information of the mobile user than periodogram method.

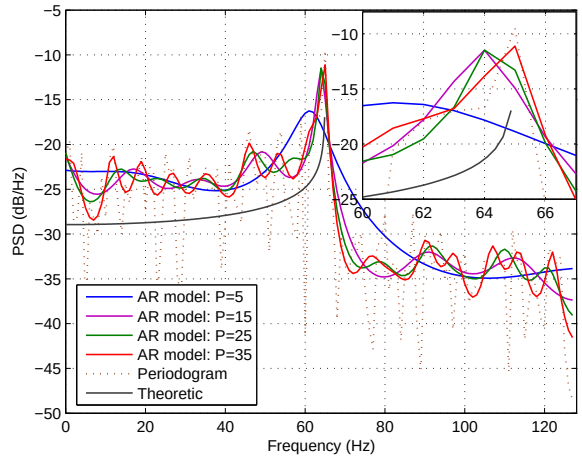

Fig. 1. PSD estimates of the received data at BS based on periodogram and AR model with different order P, and the theoretic PSD in a 2D propagation environment when $f_d = 65$ Hz, respectively. $K = 0$, $\kappa = 0$, $\alpha = 0°$, $P = \{5, 15, 25, 35\}$ and SNR $= 10$ dB.

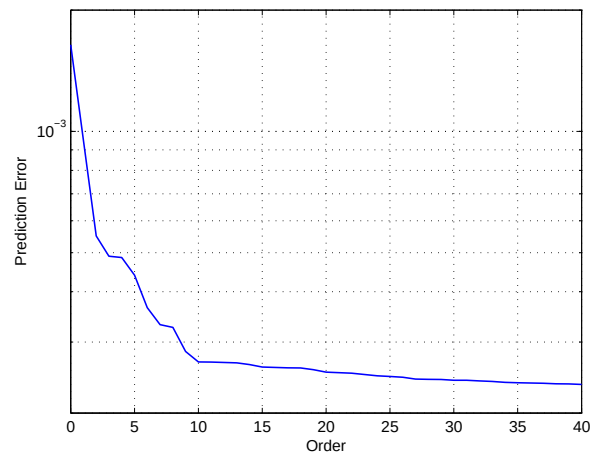

Fig. 2. Prediction error as a function of the order of AR model in a 2D propagation environment. $f_d = 65$ Hz, $K = 0$, $\kappa = 0$, $\alpha = 0°$, and SNR $=$ 10 dB.

References

[1] H. Zhang and A. Abdi, "A robust mobile speed estimator in fading channels: performance analysis and experimental results," in *Global Telecommunications Conference*, vol. 5, Nov. 2005.

[2] ——, "Space-time doppler spread estimation in mobile fading channels," in *Military Communications Conference*, Qct. 2006, pp. 1–5.

[3] W. A. Gardner, *Statistical Spectral Analysis: A Nonprobabilistic Theory*, 1st ed. Prentice Hall, 1988.

[4] S. Haykin, *Adaptive Filter Theory*, 4th ed. Prentice Hall, 2002.

[5] A. Abdi, J. A. Barger, and M. Kaveh, "A parametric model for the distribution of the angle of arrival and the associated correlation function and power spectrum at the mobile station," *IEEE Transactions on Vehicular Technology*, vol. 51, no. 3, pp. 425–434, May 2002.

[6] G. L. Stüber, *Principles of Mobile Communication*, 2nd ed. Kluwer Academic Publishers, 2001.

[7] B. Farhang-Boroujeny, *Adaptive Filters: Theory and Applications*. John Wiley & Sons, 1998.

[8] P. Stoica and R. L. Moses, *Introduction to Spectral Analysis*. Prentice Hall, 1997.

[9] A. Abdi and M. Kaveh, "Parametric modeling and estimation of the spatial characteristics of a source with local scattering," *Acoustics, Speech, and Signal Processing, 2002. Proceedings. (ICASSP '02). IEEE International Conference on*, vol. 3, pp. 2821–2824, May 2002.

[10] K. Acolatse and A. Abdi, "Efficient simulation of space-time correlated MIMO mobile fading channels," *2003. VTC 2003-Fall. 2003 IEEE 58th Vehicular Technology Conference*, vol. 1, pp. 652–656, Oct. 2003.

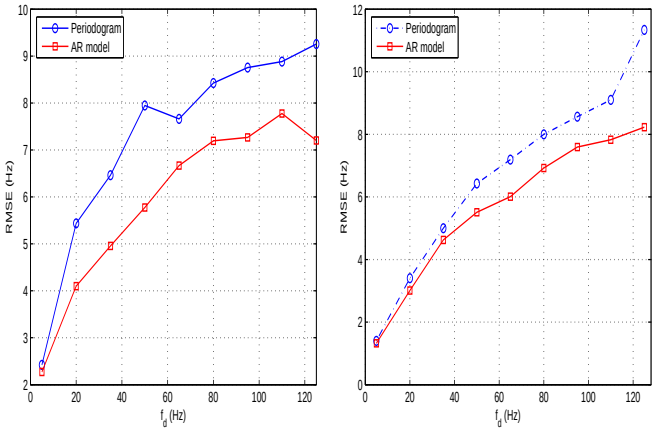

(a) $\kappa = 0$, $\alpha = 0°$. (b) $\kappa = 5$, $\alpha = 36°$.

Fig. 3. RMSE as a function of f_d over a noisy Rayleigh fading channel in a 2D propagation environment. $K = 0$, SNR $= 10$ dB, and $P = 35$.

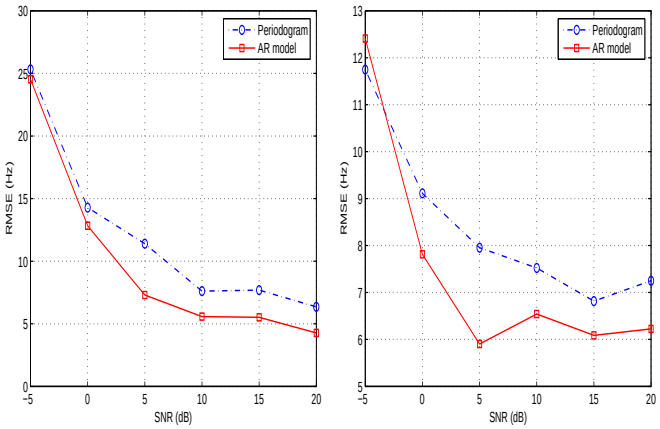

(a) $\kappa = 0$, $\alpha = 0°$. (b) $\kappa = 5$, $\alpha = 36°$.

Fig. 4. RMSE as a function of SNR over a noisy Rayleigh fading channel in a 2D propagation environment. $f_d = 65$ Hz, $K = 0$, and $P = 35$.

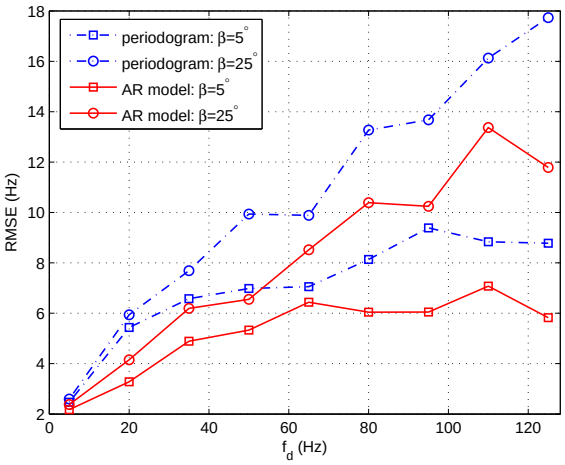

Fig. 5. RMSE as a function of f_d over a noisy Rayleigh fading channel in a 3D propagation environment. $\beta = \{5°, 25°\}$, $K = 0$, $\kappa = 0$, $\alpha = 0°$, SNR $= 10$ dB, and $P = 35$.

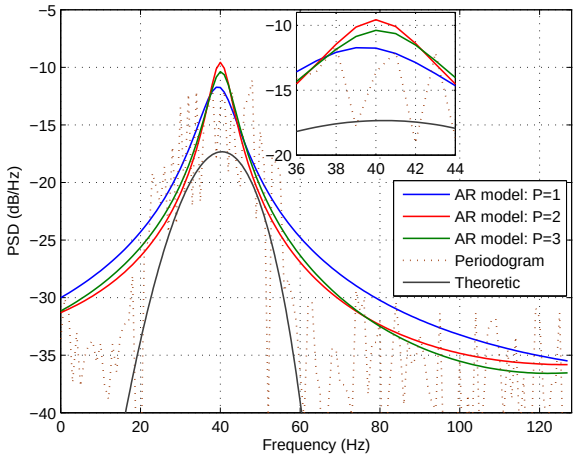

Fig. 6. PSD estimates of the received data at BS based on periodogram and AR model with different order P, and the theoretic PSD when $f_d = 80$ Hz, respectively. $K = 0$, $\kappa = 100$, $\alpha = 60°$, $P = \{1, 2, 3\}$ and SNR $= 10$ dB.

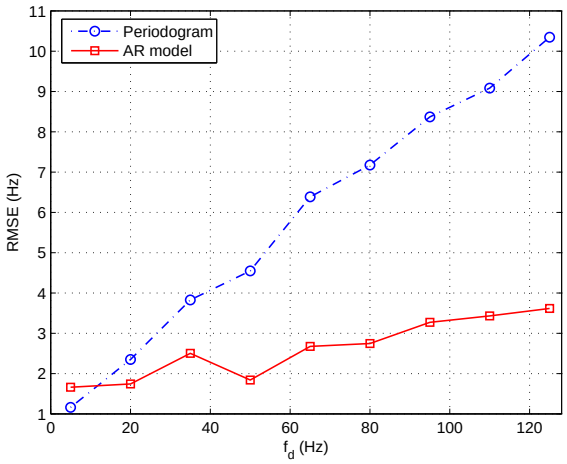

Fig. 7. RMSE as a function of f_d over a noisy Rayleigh fading channel with $L = 2$ antennas. $K = 0$, $\kappa = 100$, $\alpha = 60°$, $\Delta = 0.5$, SNR $= 10$ dB, and $P = 2$.

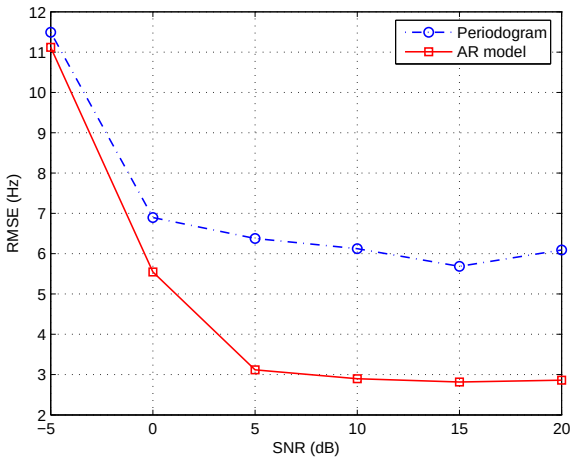

Fig. 8. RMSE as a function of SNR over a noisy Rayleigh fading channel with $L = 2$ antennas. $f_d = 65$ Hz, $K = 0$, $\kappa = 100$, $\alpha = 60°$, $\Delta = 0.5$, and $P = 2$.